

# Versatile Picklocks To Access All Opioid Receptors: Tuning the Selectivity and Functional Profile of the Cyclotetrapeptide c[Phe-D-Pro-Phe-Trp] (CJ-15,208)

Rossella De Marco,<sup>†,§</sup> Andrea Bedini,<sup>‡,§</sup> Santi Spampinato,<sup>\*,‡</sup> Lorenzo Cavina,<sup>†</sup> Edoardo Pirazzoli,<sup>†</sup> and Luca Gentilucci<sup>\*,†</sup>

<sup>†</sup>Department of Chemistry "G. Ciamician", University of Bologna, Via Selmi 2, 40126 Bologna, Italy

<sup>‡</sup>Department of Pharmacy and Biotechnology, University of Bologna, Via Irnerio 48, 40126 Bologna, Italy

**S** Supporting Information

**ABSTRACT:** Recently, the tryptophan-containing noncationizable opioid peptides emerged with atypical structure and unexpected *in vivo* activity. Herein, we describe analogs of the naturally occurring mixed  $\kappa/\mu$ -ligand c[Phe-D-Pro-Phe-Trp] **1** (CJ-15,208). Receptor affinity, selectivity, and agonism/antagonism varied upon enlarging macrocycle size, giving the  $\mu$ -agonist **9** or the  $\delta$ -antagonist **10** characterized by low nanomolar affinity. In particular, the  $\mu$ -agonist c[ $\beta$ -Ala-D-Pro-Phe-Trp] **9** was shown to elicit potent antinociception in a mouse model of visceral pain upon systemic administration.



## INTRODUCTION

The cyclotetrapeptide (CTP) c[Phe-D-Pro-Phe-Trp] **1** (CJ-15,208),<sup>1</sup> isolated from the fermentation broth of the fungus *Ctenomyces serratus* ATCC15502, came to the spotlight for its unusual opioid activity. *In vitro*, **1** was a modestly selective KOR ligand, with a  $IC_{50}$  of 47 nM, while affinities for MOR and DOR were 260 and 2600 nM, respectively, and antagonist activity against the KOR agonist asimadoline in the rabbit vas deferens smooth muscle assay was  $EC_{50} = 1300$  nM.<sup>1</sup> The antagonist behavior was confirmed by the [<sup>32</sup>S]GTP $\gamma$ S functional test.<sup>2</sup> Ala-scan highlighted the importance of the residues Phe<sup>3</sup> and Trp<sup>4</sup>; indeed, c[Ala-D-Pro-Phe-Trp] **2** (Figure 1) showed low nanomolar affinity for KOR and MOR, while the other Ala derivatives suffered a substantial loss in binding affinity.<sup>3</sup> The reversal of the configuration at Trp gave **3** (Figure 1), a dual KOR/MOR antagonist in the [<sup>32</sup>S]GTP $\gamma$ S test,  $IC_{50} = 140$  nM.<sup>2</sup> Also for **3**, Ala-scan was not

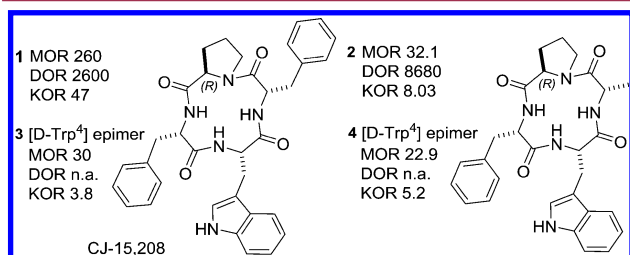


**Figure 1.** Structures of **1** and of the analogue **2** identified by Ala-scan; OR affinities ( $K_i$ , nM) of **1**, **2**, and their [D-Trp<sup>4</sup>] stereoisomers **3**, **4**.

tolerated at positions 3 and 4, since c[Ala-D-Pro-Phe-D-Trp] **4** was the only compound equipotent to **3** (Figure 1).<sup>2</sup>

All derivatives of **1** maintained the same mixed KOR > MOR affinity profile, albeit with different  $K_i$  values, and did not exhibit any agonist activity *in vitro*. *In vivo*, the Ala derivatives showed somewhat contrasting activities compared to the parent compounds. As expected, epimer **3** behaved as a KOR antagonist also *in vivo* and prevented the stress-induced reinstatement of extinguished cocaine-seeking behavior.<sup>4</sup> In contrast, the natural isomer **1** exhibited robust antinociceptive activity in the warm-water tail withdrawal test following icv administration.<sup>4</sup> Intriguingly, also the Ala analog **4** produced potent OR-mediated antinociception *in vivo*.<sup>5</sup> Finally, **1** and **3** were found to be active after oral administration and appeared to penetrate the CNS.<sup>6,7</sup>

The structures of CTP **1** and all its derivatives appear clearly correlated to that of the cyclopentapeptide (CPP) c[Phe-Gly-Tyr-D-Pro-D-Trp].<sup>8</sup> Discovered independently from **1**, the CPP was designed as a cyclic analogue of the endogenous MOR agonist H-Tyr-Pro-Trp-PheNH<sub>2</sub> endomorphin-1 (EM1).<sup>9</sup> These Trp-containing macrocycles are clearly distinct from the classic opioid peptide agonists, as they lack the protonable amino group of Tyr<sup>1</sup>, generally regarded as the fundamental "message" pharmacophore.<sup>10,11</sup> The CPP was a selective MOR ligand with a  $10^{-8}$  M affinity, acting as a partial agonist at MOR in the cAMP functional assay.<sup>8</sup> After systemic administration, it produced antinociception in a mouse model of visceral pain,<sup>12</sup> while the parent EM1 was completely ineffective.<sup>13,14</sup>

**Received:** March 20, 2016

**Published:** September 8, 2016

Subsequent modifications gave c[Phe-Gly-Tyr-Gly-D-Trp] and c[Phe-D-isoAsp- $\beta$ -Ala-D-Trp], which showed 10-fold improved MOR affinity while maintaining the agonist profile.<sup>15</sup> Experiments aimed at determining the minimal bioactive sequence identified the MOR-selective agonist tripeptide Ac-D-Trp-Phe-GlyNH<sub>2</sub>.<sup>16</sup> The introduction of different substituents at the indole of D-Trp was shown to influence BBB permeability, giving measurable central antinociception mediated by MOR in the mouse warm-water tail withdrawal assay after ip administration.<sup>17</sup>

Despite the close structural similarities, the two families of opioid peptides showed distinct receptor selectivity and in vivo activity. This led us to presume a correlation between bioactivity and 3D displays of the shared bunch of pharmacophores, which depend in turn on stereochemistry, ring size, and secondary structures. As a consequence, we designed selected analogues of the leads **1** and **2** (Figure 2), and we analyzed receptor affinity and selectivity, aiming at obtaining molecular picklocks capable of specifically interacting with MOR, DOR, or KOR.

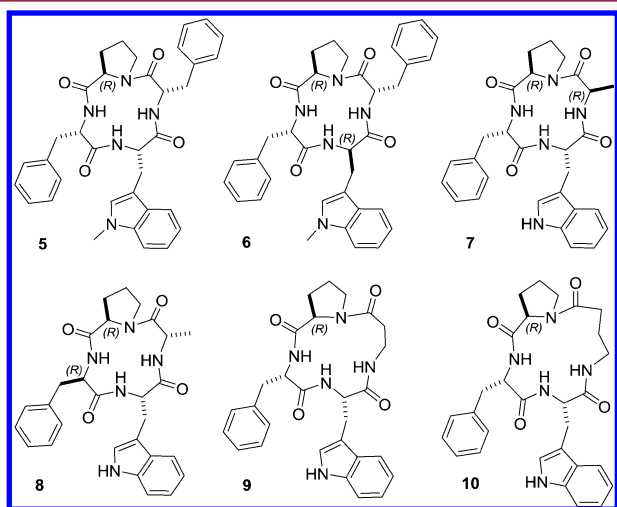


**Figure 2.** Structures of the CTPs **5–10** and analogues of **1** and **2** utilized in this study.

## RESULTS AND DISCUSSION

The analogues of **1** utilized in this study are shown in Figure 2. Previous SAR investigations<sup>2,3</sup> pointed at Trp as the

fundamental residue of the parent peptide. To better analyze the role of the indole ring of Trp, we designed the peptides c[Phe-D-Pro-Phe-(1-MeTrp)] **5** and c[Phe-D-Pro-Phe-D-(1-MeTrp)] **6**, analogues of **1** and **3**, respectively, in which the nitrogen of indole was methylated. Peptides **7** and **8** were designed as analogues of **2** characterized by the reversal of stereochemistry at residue 1 or 3. The introduction of  $\beta$ -Ala and GABA ( $\gamma$ -aminobutyric acid) in place of Ala<sup>1</sup> gave the analogues **9** and **10**, respectively, characterized by increasing macrocycle size.

The cyclopeptides of general structure c[Xaa<sup>1</sup>-D-Pro<sup>2</sup>-L-Phe/D-Phe<sup>3</sup>-Trp<sup>4</sup>] were obtained from the linear sequences H-Trp-Xaa-D-Pro-L/D-Phe-OH. Each enantiomer of 1-MeTrp was prepared as described elsewhere, by the asymmetric Friedel–Crafts alkylation of 1-methylindole with a dehydroalanine derivative equipped with a chiral auxiliary, promoted by SnCl<sub>4</sub> and phenol.<sup>18</sup> The linear peptides were prepared in turn by MW-assisted solid-phase synthesis on a Wang resin, using Fmoc-protected amino acids and HBTU/HOBt/DIPEA as activating agents. Fmoc deprotection was performed with piperidine in DMF under MW irradiation. To cleave the peptides, the resin was treated with TFA in the presence of scavengers. Peptide purities were determined to be 69–84% by reversed-phase (RP) HPLC, and their identity was checked by electrospray ionization mass spectrometry (ESI MS) (Table S1).

Cyclization was performed without prior purifications by slow addition of the crude linear peptides to a solution of HATU/DIPEA in DMF at rt, using a temporized syringe to achieve pseudo-high-dilution conditions.<sup>3,19</sup> The cyclic peptides were isolated by semipreparative RP HPLC, and purities were determined to be 95–98% by RP HPLC (Table S1) and elemental analysis. The identity of the compounds was confirmed by ESI MS, <sup>1</sup>H NMR, 2D gCOSY, and <sup>13</sup>C NMR analyses. The CTPs **7** and **8** were recovered in lower yields as compared to **5** and **6**, suggesting the optimality of the stereochemistry pattern of the native compound. In particular, the reaction of H-Trp-Ala-D-Pro-D-Phe-OH under the conditions described above gave the desired **8** only in traces. The yield was increased to a moderate 55% starting from the alternative precursor H-Ala-D-Pro-D-Phe-Trp-OH in the presence of 10 equiv of NaHCO<sub>3</sub> to assist in the macrocyclization of the peptide and heating the reaction mixture by MW irradiation (45 °C) for 10 min before quenching. The 13- and 14-membered analogues **9** and **10** were obtained in almost quantitative yields (Table S1). This was not unexpected; CTPs

**Table 1.** In Vitro OR Affinities of the CTPs and Reference Compounds for hORs<sup>a</sup>

compd	sequence	K <sub>i</sub> (nM) <sup>a</sup>		
		MOR	DOR	KOR
DAMGO	H-Tyr-D-Ala-Gly-NMePhe-Glyol	1.5 ± 0.1		
DPDPE	H-Tyr-c[D-Pen-Gly-Phe-D-Pen]-OH		3.30 ± 0.05	
U50,488	nonpeptide			2.90 ± 0.04
<b>1</b>	c[Phe-D-Pro-Phe-Trp]	127 ± 13	>10 <sup>5</sup>	32 ± 4
<b>5</b>	c[Phe-D-Pro-Phe-(1-MeTrp)]	<i>b</i>	>10 <sup>5</sup>	>10 <sup>5</sup>
<b>6</b>	c[Phe-D-Pro-Phe-D-(1-MeTrp)]	>10 <sup>5</sup>	>10 <sup>5</sup>	>10 <sup>5</sup>
<b>7</b>	c[D-Ala-D-Pro-Phe-Trp]	>10 <sup>5</sup>	>10 <sup>5</sup>	>10 <sup>5</sup>
<b>8</b>	c[Ala-D-Pro-D-Phe-Trp]	>10 <sup>5</sup>	>10 <sup>5</sup>	>10 <sup>5</sup>
<b>9</b>	c[ $\beta$ -Ala-D-Pro-Phe-Trp]	4.1 ± 1.2	>10 <sup>5</sup>	>10 <sup>5</sup>
<b>10</b>	c[GABA-D-Pro-Phe-Trp]	<i>b</i>	3.08 ± 0.05	>10 <sup>5</sup>

<sup>a</sup>Mean of 4–6 determinations ± SE. <sup>b</sup>Radioligand displacement <50% up to 10<sup>-2</sup> M.

composed of all  $\alpha$ -amino acids may be difficult to synthesize, due to the highly constrained conformation required for cyclization.<sup>20</sup> In contrast, the introduction of  $\beta$ - or  $\gamma$ -residues renders the structures easier to synthesize and conformationally more stable.<sup>20–22</sup>

**Binding Affinity to Human ORs.** To evaluate compounds' affinity toward the ORs, displacement binding assays were performed in HEK-293 cells expressing the cloned human (h) MOR, DOR, or KOR, using [<sup>3</sup>H]DAMGO, [<sup>3</sup>H]-diprenorphine, or [<sup>3</sup>H]U69,593 as specific radioligands, respectively. The reference compounds DAMGO, DPDPE, and U50,488<sup>23</sup> (Figure S3), showed  $K_i$  values in the nM range and high selectivity to the respective receptors (Table 1), as expected (Supporting Information). The parent **1** displayed KOR > MOR affinity consistent with that previously reported.<sup>1–3</sup> As it regards the analogues, they showed a wide range of different affinity and selectivity (Table 1).

The CTPs **5** and **6**, which include L-(1-MeTrp) or D-(1-MeTrp) in their sequence, showed null or negligible OR affinity. These findings highlighted the importance of indole NH in peptide/receptor interaction.<sup>15,24</sup> Peptides **7** and **8** did not show any significant receptor affinity, confirming the relevance of the relative 3D display of the pharmacophores, since **7** and **8** share the same sequence as the potent KOR/MOR ligand **2**,<sup>3</sup> with inverted configuration at residue 1 or 3. In contrast, the introduction of  $\beta$ -Ala in place of Ala<sup>1</sup> yielded the 13-membered CTP **9**, a highly selective MOR ligand ( $K_i = 4.1$  nM, Table 1). Surprisingly, a further enlargement of ring size by introducing GABA at position 1 determined a different receptor selectivity: the 14-membered **10** showed very little affinity to MOR and gained a noteworthy DOR affinity ( $K_i = 3.08$  nM, Table 1).

**Conformational Analysis.** To shed light on the different receptor selectivity of the CTPs, the backbone conformations of the KOR > MOR ligand **1**, the MOR-selective **9**, and the DOR  $\gg$  MOR **10** were investigated in solution by NMR analysis and molecular dynamics simulations (MD). <sup>1</sup>H NMR spectroscopy was performed in 8:2 mixtures of [D<sub>6</sub>]dimethyl sulfoxide (DMSO) and H<sub>2</sub>O, recommended as excellent representative of biological fluids for the analysis of opioid peptides.<sup>25,26</sup> For all compounds but **9**, the spectra showed a single set of resonances, suggestive of conformational homogeneity or a rapid equilibrium between conformers. In contrast, **9** showed two distinct sets of sharp resonances at about 2:1 ratio (Supporting Information). This CTP appeared as a single peak in RP and direct HPLC under different conditions, likely excluding the possibility to separate the two conformers (Supporting Information).

Variable-temperature (VT) NMR experiments were used to detect if amide protons were involved in intramolecular hydrogen-bonding or were solvent-exposed. The  $\Delta\delta/\Delta t$  parameters of **1** (Table 2) revealed that the amide protons Phe<sup>3</sup>NH and Trp<sup>4</sup>NH were nearly completely insensitive to

increasing temperature (for both,  $\Delta\delta/\Delta t = -0.8$  ppb/K), suggesting the plausible occurrence of conformations having Phe<sup>3</sup>NH and Trp<sup>4</sup>NH involved in very strong hydrogen bonds. In contrast, the analysis of the major conformer **9A** indicated a strong hydrogen bond on TrpNH ( $-1.0$  ppb/K). The minor conformer **9B** and **10** did not show evidence of strong hydrogen bonding. However, the comparison of the  $\Delta\delta/\Delta t$  parameters was suggestive of significant populations of conformers stabilized by a hydrogen bond on  $\beta$ -AlaNH for **9B** ( $-2.0$  ppb/K) and GABANH for **10** ( $-2.4$  ppb/K).

Subsequently, the model compounds were analyzed by 2D-ROESY in DMSO-*d*<sub>6</sub>/H<sub>2</sub>O (8:2). Cross-peaks intensities were ranked to infer plausible interproton distances (Supporting Information). Structures consistent with the spectroscopic analyses were obtained by restrained MD simulations,<sup>27</sup> using the ROESY-derived distances as constraints, and minimized with AMBER<sup>28</sup> force field. Simulations were conducted in a box of explicit water molecules starting from a set of random structures.<sup>27</sup> The structures were subjected to high-temperature restrained MD with a scaled force field, followed by a simulation with full restraints. The system was gradually cooled, and the structures were minimized<sup>28</sup> and clustered by the rmsd analysis of the backbone atoms. The conformers **9A** and **9B** were analyzed separately. For all compounds, this procedure gave one major cluster comprising the large majority of the structures. The representative structures with the lowest energy and the least number of restraint violations were selected and analyzed (Figure 3). To analyze the dynamic behavior of the peptides, the structures were subjected to unrestrained MD simulations in a box of water at rt.

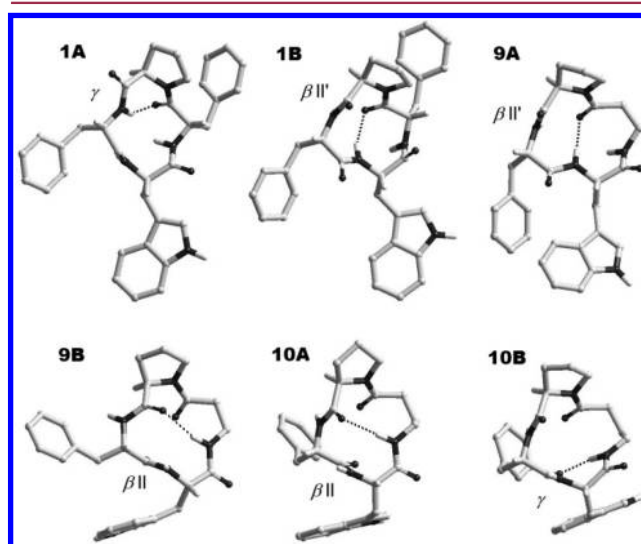


**Figure 3.** Representative conformers of the CTPs **1**, **9**, and **10**. For clarity, only  $\alpha$  and NH hydrogens are shown.

**Table 2.**  $\Delta\delta/\Delta t$  Values (ppb/K) for the Amide Protons of **1**, **9** (Conformers A and B), and **10** in 8:2 DMSO-*d*<sub>6</sub>/H<sub>2</sub>O

compd	sequence	NH <sup>1</sup>	NH <sup>3</sup>	NH <sup>4</sup>
<b>1</b>	c[Phe <sup>1</sup> -D-Pro <sup>2</sup> -Phe <sup>3</sup> -Trp <sup>4</sup> ]	-1.5	-0.8	-0.8
<b>9A</b>	c[ $\beta$ -Ala <sup>1</sup> -D-Pro <sup>2</sup> -Phe <sup>3</sup> -Trp <sup>4</sup> ]	-3.3	-5.0	-1.0
<b>9B</b>		-2.0	-4.2	-4.1
<b>10</b>	c[GABA <sup>1</sup> -D-Pro <sup>2</sup> -Phe <sup>3</sup> -Trp <sup>4</sup> ]	-2.4	-5.9	-6.2

In the structure **1A**, D-Pro<sup>2</sup> was embedded into a  $\gamma$ -turn stabilized by the explicit hydrogen bond Phe<sup>3</sup>NH-Phe<sup>1</sup>C=O. This structure ( $\gamma$ @D-Pro<sup>2</sup>) accounted for the hydrogen bond on Phe<sup>3</sup>NH predicted by VT-NMR. On the other hand, the analysis of the trajectories of the unrestrained MD simulations revealed the alternative structure **1B** (Figure 3), characterized by an inverse type II  $\beta$ -turn centered on D-Pro<sup>2</sup>-Phe<sup>3</sup> ( $\beta$ II'@D-Pro<sup>2</sup>-Phe<sup>3</sup>), stabilized by the hydrogen bond Trp<sup>4</sup>NH-PheC=O, in agreement with the temperature coefficient of TrpNH.

The conformers **A** and **B** of **9** differed in the opposite orientation of the amide bond between Phe<sup>3</sup> and Trp<sup>4</sup>. Therefore, **9A** adopted an inverse type II  $\beta$ -turn on D-Pro<sup>2</sup>-Phe<sup>3</sup> ( $\beta$ II'@D-Pro<sup>2</sup>-Phe) with the hydrogen bond Trp<sup>4</sup>NH-GABA<sup>1</sup>C=O, while **9B** was characterized by a regular type II  $\beta$ -turn on Phe<sup>3</sup>-Trp<sup>4</sup> ( $\beta$ II@Phe<sup>3</sup>-Trp<sup>4</sup>) and the hydrogen bond  $\beta$ -Ala<sup>1</sup>NH-D-Pro<sup>2</sup>C=O, confirming the results of VT NMR (Figure 3). Both conformers were found highly stable during the unrestrained MD simulations, and interconversion was not observed, possibly explaining the occurrence of two sets of distinct NMR resonances. Finally, the structure of **10** did not show any hydrogen bond. Nevertheless, the analysis of the MD trajectories revealed an equilibrium between the  $\beta$ II@Phe<sup>3</sup>-Trp<sup>4</sup> conformer **A** (Figure 3), stabilized by the hydrogen bond GABA<sup>1</sup>NH-D-Pro<sup>2</sup>C=O, and the  $\gamma$ @Trp<sup>4</sup> conformer **B**, the latter with the hydrogen bond Phe<sup>3</sup>C=O-GABA<sup>1</sup>NH, consistent with the VT-NMR data.

The comparison of the 3D structures in Figure 3 suggested that the different receptor selectivity of **1**, **9**, and **10** might depend on the alternative backbone secondary structures. Despite of the occurrence of the two conformers  $\beta$ II'@D-Pro<sup>2</sup>-Phe<sup>3</sup> **A** and  $\beta$ II@Phe<sup>3</sup>-Trp<sup>4</sup> **B**, **9** was a potent and selective MOR ligand. Docking studies aimed at investigating the poses of the two conformers within the crystal structure of MOR in the active state will be performed in due course. At present, it could be supposed that the predominant KOR affinity of **1** might be correlated to the  $\gamma$ @D-Pro<sup>2</sup> conformer **A**, while the second conformer  $\beta$ II'@D-Pro<sup>2</sup>-Phe<sup>3</sup> **B** would be responsible for the significant MOR affinity. As for the DOR > MOR ligand **10**, the coexistence of the two conformers  $\gamma$ @Trp<sup>4</sup> **B** and  $\beta$ II@Phe<sup>3</sup>-Trp<sup>4</sup> **A** would explain the preferential DOR affinity of **10** and its residual ability to bind to MOR.

**Pharmacological Characterization of 9 and 10.** The functional activity of the potent and selective MOR ligand **9** and of the DOR  $\gg$  MOR ligand **10**, was investigated by the cAMP test in whole HEK-293 cells stably expressing hMOR (HEK/MOR) or hDOR (HEK/DOR). The reference compounds morphine and DAMGO for HEK/MOR, and DPDPE for HEK/DOR, significantly inhibited forskolin-induced cAMP accumulation, with IC<sub>50</sub> values of 4.3, 19, and 1.6 nM and E<sub>max</sub> (the maximal obtainable effect) of 77%, 95%, and 89%, respectively (Table 3), as expected (Supporting Information).

The MOR-specific **9** inhibited forskolin-induced cAMP accumulation, with IC<sub>50</sub> = 6.1 nM and E<sub>max</sub> = 90%, suggestive of a full agonist behavior (Table 3). The DOR  $\gg$  MOR ligand **10** inhibited forskolin-induced cAMP accumulation in HEK/

MOR, albeit with a worse IC<sub>50</sub> (183 nM; Table 3). Interestingly, **10** did not alter forskolin-induced cAMP accumulation in HEK/DOR but significantly antagonized in a concentration-related manner the inhibition of forskolin-induced cAMP accumulation by 10  $\mu$ M DPDPE (Table 3), with IC<sub>50</sub> = 7.4 nM.

Considering that **1** is well-known to have KOR antagonist properties and its analogs have been reported with antagonist effects at the MOR and DOR as well, the ability of **9** to counteract DAMGO-, DPDPE-, or U50,488-mediated inhibition of forskolin-induced cAMP accumulation was investigated. Nevertheless, **9** did not display any antagonist activity (data not shown); similarly, **10** did not alter DAMGO activity at MOR and U50,488 activities at KOR (data not shown).

Albeit accompanied by severe side effects, MOR agonists are still the most potent and widely used analgesics. For this reason, on prosecuting a program dedicated to the discovery of new opioid peptides showing analgesic activity in vivo,<sup>12,13,17,29,30</sup> we turned our attention to the potent and selective MOR agonist **9**. Preliminarily, incubation in mouse serum for 3 h (Supporting Information)<sup>12</sup> allowed confirming the enzymatic stability of **9**, as generally observed for bioactive cyclopeptides,<sup>31,32</sup> including **1** and **3**.<sup>6,7</sup> Subsequently, the peripheral preemptive antinociceptive effect elicited by **9** was determined in a mouse model of visceral pain, as previously reported.<sup>12</sup> Mice were injected with 0.6% AcOH into the peritoneal cavity, thus triggering abdominal stretching combined with an exaggerated extension of the hindlimbs. Animals treated with vehicle 5 min prior to AcOH challenge displayed an average of 35.0  $\pm$  5.5 abdominal writhes during the 10 min observation after injection. On the contrary, when given 5 min before AcOH challenge, **9** (0.5–10 mg/kg ip) produced a dose-related decrease in the number of abdominal writhes evoked by AcOH (Figure 4), ED<sub>50</sub> = 0.64  $\pm$  0.06 mg/

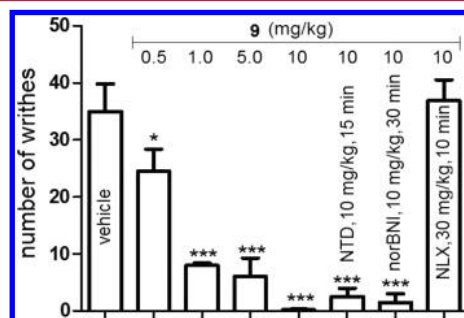


**Figure 4.** Effect of **9** on the number of writhes produced by AcOH. Vehicle or **9** was administered ip 5 min before ip injection of AcOH. DOR antagonist NTD, KOR antagonist norBNI, and not selective antagonist NLX were ip administered at the indicated doses 15, 30, or 10 min prior to **9**, respectively. Data are the mean  $\pm$  SEM of 6–8 mice/group: (\*)  $p$  < 0.05 vs mice treated with vehicle alone; (\*\*\*)  $P$  < 0.001 vs mice treated with vehicle alone or with naloxone + **9** (Dunnett multiple comparison test after ANOVA).

**Table 3.** Inhibitory Effects of **9** and **10** on Forskolin-Induced cAMP Formation in HEK/MOR and of **10** (Alone or Coadministered with DPDPE) in HEK/DOR

compd	IC <sub>50</sub> (nM) <sup>a</sup>	E <sub>max</sub> (% vehicle) <sup>a</sup>
morphine (HEK/MOR)	4.3 $\pm$ 0.4	77 $\pm$ 4
DAMGO (HEK/MOR)	19.3 $\pm$ 1.1	95 $\pm$ 4
DPDPE (HEK/DOR)	1.6 $\pm$ 0.3	89 $\pm$ 3
<b>9</b> (HEK/MOR)	6.1 $\pm$ 0.3	90 $\pm$ 5
<b>10</b> (HEK/MOR)	183 $\pm$ 47	82 $\pm$ 4
<b>10</b> (HEK/DOR)	<sup>b</sup>	
inhibition of DPDPE (10 $\mu$ M) activity by <b>10</b> (HEK/DOR)	7.4 $\pm$ 0.3	

<sup>a</sup>Mean  $\pm$  SE of 5–6 independent experiments performed in triplicate.

<sup>b</sup>**10** (10<sup>-12</sup>–10<sup>-4</sup> M) did not alter forskolin-induced cAMP formation.

kg. Interestingly, **9**-mediated antinociceptive effect was counteracted by pretreating the animals with the opioid antagonist NLX (30 mg/kg, ip) but not by the DOR selective antagonist NTD (10 mg/kg, ip) or by the KOR selective antagonist norBNI (10 mg/kg, ip), thus confirming that the observed effect is MOR-dependent and does not involve any other opioid receptor such as peripherally expressed KOR. Antinociception elicited by **9** would not affect behavioral

responses; in fact, administered at analgesic doses, **9** did not cause (within 6 h) any significant alteration of spontaneous locomotor activity or circling behavior, Straub tail, or grooming (data not shown).

## CONCLUSIONS

The CTP **1** and correlated peptides,<sup>1–8,15–17</sup> including **9** and **10**, constitute the new family of the tryptophan-containing noncationizable opioid peptides (in short, TryCoNCOPs). In contrast to most opioids, their atypical bioactivity resides in the minimal pharmacophoric motif Trp&Phe, with indole NH fundamental to ligand–receptor interaction. As a bunch of picklocks, the cyclopeptides permit easy access to all ORs. The significant preference of **9**, **10**, and **1** for MOR, DOR, and KOR, respectively, seems to be correlated to specific  $\gamma$ - or  $\beta$ -turn secondary structures. The MOR-selective ligand **9** revealed full agonist activity in vitro, while **10** displayed significant preference for DOR over MOR, acting as a strong DOR antagonist and a weak agonist at MOR. Interestingly, **9** revealed a strong, MOR-dependent antinociceptive effect in vivo upon systemic administration, consistent with the cyclic nature.<sup>31,32</sup> It is well acknowledged that peripheral and central MOR may contribute to modulate visceral pain.<sup>33–35</sup> Thus, both sites may contribute to analgesia elicited by **9**. We plan to better address this aspect in future investigations.

## EXPERIMENTAL SECTION

**General Methods.** Chemicals, biological reagents, disposables, cells, and animals were purchased from commercial sources. The MW-assisted synthesis was performed at 40 W, using a MicroSYNTH microwave lab station, monitoring the internal temperature with a built-in ATC-FO advanced fiber optic automatic temperature control. Purities were determined to be >95% by RP HPLC and elemental analysis. Analytical RP HPLC was performed on an Agilent 1100 apparatus, using a C18 column Phenomenex Gemini 3  $\mu$ m C18 110 Å 100 3 3.0 mm, mobile phase from 9:1 H<sub>2</sub>O/CH<sub>3</sub>CN to 2:8 H<sub>2</sub>O/CH<sub>3</sub>CN (plus 0.1% HCOOH for the linear peptides) in 20 min at a flow rate of 1.0 mL min<sup>-1</sup>. Direct-phase HPLC analysis was done on a Kromasil 60-5 Diol column, mobile phase hexane/2-propanol 60:40, at a flow rate of 0.6 mL min<sup>-1</sup>. Semipreparative RP HPLC was performed on a C18 RP column ZORBAX Eclipse XDBC18 PrepHT cartridge 21.2 3 150 mm 7  $\mu$ m, mobile phase from 8:2 H<sub>2</sub>O–CH<sub>3</sub>CN to 100% CH<sub>3</sub>CN, in 10 min, flow rate 12 mL min<sup>-1</sup>. ESI analysis was performed using a MS single quadrupole HP 1100MSD detector. Elemental analyses were performed using a Thermo Flash 2000 CHNS/O analyzer. <sup>1</sup>H NMR spectra were recorded using a Varian Gemini apparatus at 400 MHz in 5 mm tubes in 8:2 DMSO-*d*<sub>6</sub>/H<sub>2</sub>O, water suppression by presaturation. <sup>13</sup>C NMR spectra were recorded at 100 MHz. Chemical shifts are reported as  $\delta$  values relative to residual DMSO  $\delta$  H (2.50 ppm). More details are in the [Supporting Information](#).

**CTP Synthesis.**<sup>16,17</sup> The linear peptides were assembled on a Phe-preloaded Wang resin (0.5 g, Phe loading 0.4–0.8 mmol/g). Fmoc deprotection was performed with 20% piperidine in DMF (5 mL) for 2 min under MW irradiation. Fmoc-protected amino acids (0.6 mmol) in DMF (5 mL) were coupled using TBTU/HOBt/DIPEA (0.6/0.6/1.2 mmol) while bubbling N<sub>2</sub> for 10 min under MW irradiation. Peptide cleavage was done with TFA/TIPS/water/PhOH (7:1:1:1 v/v, 15 mL), for 2 h at rt. The crude peptides which precipitated in ice-cold Et<sub>2</sub>O (69–84% pure by RP HPLC) were utilized for cyclization without further purifications. Peptides (0.1 mmol) in DMF (5 mL) were added over 12 h using a temporized syringe to HATU/DIPEA (0.4/1.0 mmol) in DMF (20 mL). After an additional 12 h of stirring, the crude CTPs were isolated by semipreparative RP HPLC (>95% pure by analytical RP HPLC and elemental analysis). For full

experimental details and analytical characterizations, see the [Supporting Information](#).

**Displacement binding assays** were performed in triplicate in HEK-293 cells stably expressing the hORs, using [<sup>3</sup>H]DAMGO, [<sup>3</sup>H]-diprenorphine, and [<sup>3</sup>H]U69,593 ([Figure S3](#)), to label MOR, DOR, or KOR, as radioligands.<sup>8,15–17</sup> In brief, compounds were incubated at 25 °C for 90 min in 100 mM Tris-HCl buffer and 0.3% BSA on cell membranes in the concentration range 10<sup>-12</sup>–10<sup>-4</sup> M; nonspecific binding was determined in the presence of the cold ligands. Cells lysed with 1 N NaOH were left in scintillation fluid for 8 h before counting. The radioactivity trapped on filters presoaked with 0.3% polyethylenimine was determined by liquid scintillation. K<sub>i</sub> values were calculated using the Cheng–Prusoff equation from the IC<sub>50</sub>. Full details are given in the [Supporting Information](#).

**cAMP Test of **9** and **10**.** The agonist activity was determined in triplicate by measuring the inhibition of forskolin-stimulated cAMP accumulation in whole HEK/MOR and HEK/DOR cells.<sup>12</sup> Cells were incubated in serum-free medium containing 0.5 mM 3-isobutyl-1-methylxanthine and exposed for 15 min to 10  $\mu$ M forskolin without and with **9** or **10** (0.001 nM to 100  $\mu$ M) at 37 °C. cAMP concentration was determined using a cAMP EIA kit. To evaluate **10** antagonist activity, HEK/DOR cells were incubated in serum-free medium containing 0.5 mM 3-isobutyl-1-methylxanthine and exposed for 15 min to 10  $\mu$ M forskolin without and with 10  $\mu$ M DPDPE and **10** (0.001 nM–100  $\mu$ M) at 37 °C. See also the [Supporting Information](#).

**Visceral Pain Test** (approved Prot. no. 29-IX/9, July 25, 2012). In summary, antinociception was evaluated in treated or control mice by counting stretching or writhing responses during 10 min after ip injection of 0.6% w/v AcOH in water (0.1 mL/10 g).<sup>12,17</sup> CTP **9**, opioid antagonists, or vehicle was administered before AcOH. Data are expressed as mean  $\pm$  SEM. Statistical significance was estimated by a mixed two-factor analysis of variance (ANOVA) or by one-way ANOVA and Dunnett post hoc test.  $p \leq 0.05$  was accepted as significant. See also the [Supporting Information](#).

**Conformational Analysis.**<sup>15,22,24</sup> 2D ROESY experiments were performed in DMSO-*d*<sub>6</sub>/H<sub>2</sub>O (8:2). Cross-peak intensities were classified as very strong, strong, medium, and weak and were associated with distances of 2.3, 2.7, 3.3, and 5.0 Å, respectively.<sup>15,24</sup> These distances were utilized as constraints in the MD simulations.<sup>27</sup> The absence of H $\alpha$ (*i*)–H $\alpha$ (*i*+1) cross-peaks reasonably excluded cis peptide bonds, so the  $\omega$  bonds were set at 180°. The restrained MD was conducted using the AMBER force field in a 30 Å  $\times$  30 Å  $\times$  30 Å box of standard TIP3P models of equilibrated water.<sup>27</sup> 50 random structures were subjected to a 50 ps restrained MD with a 50% scaled force field at 1200 K, followed by 50 ps with full restraints, after which the system was cooled in 20 ps to 50 K. The resulting structures were minimized, and backbones were clustered by the rmsd analysis.<sup>27</sup> Unrestrained MD simulations<sup>27</sup> were conducted for 10 ns at 298 K using periodic boundary conditions ([Supporting Information](#)).

## ASSOCIATED CONTENT

### Supporting Information

The Supporting Information is available free of charge on the ACS Publications website at DOI: 10.1021/acs.jmedchem.6b00420.

Full experimental details, analytical characterization of the linear precursors and of CTPs, ROESY cross peaks ([PDF](#))

Molecular formula strings and some data ([CSV](#))

Structure information ([PDB](#))

Structure information ([PDB](#))

Structure information ([PDB](#))

Structure information ([PDB](#))

Structure information ([PDB](#))

Structure information ([PDB](#))

## ■ AUTHOR INFORMATION

## Corresponding Authors

\*S.S.: e-mail, [santi.spampinato@unibo.it](mailto:santi.spampinato@unibo.it); phone, +39 0512091851.

\*L.G.: e-mail, [luca.gentilucci@unibo.it](mailto:luca.gentilucci@unibo.it); phone, +39 0512099570; fax, +39 0512099456; Web, <http://www.ciam.unibo.it/gentilucci>.

## Author Contributions

<sup>§</sup>R.D.M. and A.B. contributed equally.

## Notes

The authors declare no competing financial interest.

## ■ ACKNOWLEDGMENTS

University of Bologna, FARB (FFBO 125290), MIUR (PRIN 2010), Fondazione Veronesi-Milano (Proj. Tryptoids) are acknowledged for financial support.

## ■ ABBREVIATIONS USED

MOR, DOR, KOR,  $\mu$ -,  $\delta$ -,  $\kappa$ -opioid receptor; CTP, cyclo-tetrapeptide; CPP, cyclopentapeptide; MW, microwave;  $\beta$ -Ala,  $\gamma$ -aminopropanoic acid; DIPEA, diisopropylethylamine; HOBt, hydroxybenzotriazole; HBTU, *O*-benzotriazole-*N,N,N',N'*-tetramethyluronium hexafluorophosphate; HATU, 1-[bis-(dimethylamino)methylene]-1*H*-1,2,3-triazolo[4,5-*b*]-pyridinium 3-oxide hexafluorophosphate; RP, reversed phase; SEM, standard error of the mean;  $E_{max}$ , maximal obtainable effect; norBNI, norbinaltorphimine; NLX, naloxone; NTD, naltrindole

## ■ REFERENCES

- (1) Saito, T.; Hirai, H.; Kim, Y. J.; Kojima, Y.; Matsunaga, Y.; Nishida, H.; Sakakibara, T.; Suga, O.; Sujaku, T.; Kojima, N. CJ-15,208, a novel kappa opioid receptor antagonist from a fungus, *Ctenomyces serratus* ATCC15502. *J. Antibiot.* **2002**, *55*, 847–854.
- (2) Dolle, R. E.; Michaut, M.; Martinez-Teipel, B.; Seida, P. R.; Ajello, C. W.; Muller, A. L.; DeHaven, R. N.; Carroll, P. J. Nascent structure-activity relationship study of a diastereomeric series of kappa opioid receptor antagonists derived from CJ-15,208. *Bioorg. Med. Chem. Lett.* **2009**, *19*, 3647–3650.
- (3) Aldrich, J. V.; Kulkarni, S. S.; Senadheera, S. N.; Ross, N. C.; Reilley, K. J.; Eans, S. O.; Ganno, M. L.; Murray, T. F.; McLaughlin, J. P. Unexpected opioid activity profiles of analogues of the novel peptide kappa opioid receptor ligand CJ-15,208. *ChemMedChem* **2011**, *6*, 1739–1745.
- (4) Ross, N. C.; Reilley, K. J.; Murray, T. F.; Aldrich, J. V.; McLaughlin, J. P. Novel opioid cyclic tetrapeptides: Trp isomers of CJ-15,208 exhibit distinct opioid receptor agonism and short-acting kappa opioid receptor antagonism. *Br. J. Pharmacol.* **2012**, *165*, 1097–1108.
- (5) Aldrich, J. V.; Senadheera, S. N.; Ross, N. C.; Reilley, K. A.; Ganno, M. L.; Eans, S. E.; Murray, T. F.; McLaughlin, J. P. Alanine analogues of [D-Trp]CJ-15,208: novel opioid activity profiles and prevention of drug- and stress-induced reinstatement of cocaine-seeking behavior. *Br. J. Pharmacol.* **2014**, *171*, 3212–3222.
- (6) Aldrich, J. V.; Senadheera, S. N.; Ross, N. C.; Ganno, M. L.; Eans, S. O.; McLaughlin, J. P. The macrocyclic peptide natural product CJ-15,208 is orally active and prevents reinstatement of extinguished cocaine-seeking behavior. *J. Nat. Prod.* **2013**, *76*, 433–438.
- (7) Eans, S. O.; Ganno, M. L.; Reilley, K. J.; Patkar, K. A.; Senadheera, S. N.; Aldrich, J. V.; McLaughlin, J. P. The macrocyclic tetrapeptide [D-Trp]CJ-15,208 produces short-acting kappa opioid receptor antagonism in the CNS after oral administration. *Br. J. Pharmacol.* **2013**, *169*, 426–436.
- (8) Cardillo, G.; Gentilucci, L.; Tolomelli, A.; Spinosa, R.; Calienni, M.; Qasem, A. R.; Spampinato, S. Synthesis and evaluation of the affinity toward  $\mu$ -opioid receptors of atypical, lipophilic ligands based

on the sequence c[Tyr-Pro-Trp-Phe-Gly]. *J. Med. Chem.* **2004**, *47*, 5198–5203.

(9) Zadina, J. E.; Hackler, L.; Ge, L. J.; Kastin, A. J. A potent and selective endogenous agonist for the  $\mu$ -opioid receptor. *Nature* **1997**, *386*, 499–502.

(10) Gentilucci, L.; Squassabia, F.; Artali, R. Re-discussion of the importance of ionic interactions in stabilizing ligand-opioid receptor complex and in activating signal transduction. *Curr. Drug Targets* **2007**, *8*, 185–196.

(11) Gentilucci, L.; Tolomelli, A.; De Marco, R.; Artali, R. Molecular docking of opiates and opioid peptides, a tool for the design of selective agonists and antagonists, and for the investigation of atypical ligand-receptor interactions. *Curr. Med. Chem.* **2012**, *19*, 1587–1601.

(12) Bedini, A.; Baiula, M.; Gentilucci, L.; Tolomelli, A.; De Marco, R.; Spampinato, S. Peripheral antinociceptive effects of the cyclic endomorphin-1 analog c[YpwFG] in a mouse visceral pain model. *Peptides* **2010**, *31*, 2135–2140.

(13) Spampinato, S.; Qasem, A. R.; Calienni, M.; Murari, G.; Gentilucci, L.; Tolomelli, A.; Cardillo, G. Antinociception by a peripherally administered novel endomorphin-1 analogue containing  $\beta$ -proline. *Eur. J. Pharmacol.* **2003**, *469*, 89–95.

(14) Fichna, J.; Janecka, A.; Costentin, J.; Do Rego, J. C. The endomorphin system and its evolving neurophysiological role. *Pharmacol. Rev.* **2007**, *59*, 88–123.

(15) Gentilucci, L.; Tolomelli, A.; De Marco, R.; Spampinato, S.; Bedini, A.; Artali, R. The inverse type II beta-turn on D-Trp-Phe, a pharmacophoric motif for MOR agonists. *ChemMedChem* **2011**, *6*, 1640–1653.

(16) De Marco, R.; Tolomelli, A.; Spampinato, S.; Bedini, A.; Gentilucci, L. Opioid activity profiles of oversimplified peptides lacking in the protonable *N*-terminus. *J. Med. Chem.* **2012**, *55*, 10292–10296.

(17) De Marco, R.; Bedini, A.; Spampinato, S.; Gentilucci, L. Synthesis of tripeptides containing D-Trp substituted at the indole ring, assessment of opioid receptor binding and in vivo central antinociception. *J. Med. Chem.* **2014**, *57*, 6861–6866.

(18) De Marco, R.; Cavina, L.; Greco, A.; Gentilucci, L. Easy preparation of dehydroalanine building blocks equipped with oxazolidin-2-one chiral auxiliaries, and applications to the stereoselective synthesis of substituted tryptophans. *Amino Acids* **2014**, *46*, 2823–2839.

(19) Malesevic, M.; Strijowski, U.; Bächle, D.; Sewald, N. An improved method for the solution cyclization of peptides under pseudo-high dilution conditions. *J. Biotechnol.* **2004**, *112*, 73–77.

(20) De Leon Rodriguez, L. M.; Weidkamp, A. J.; Brimble, M. A. An update on new methods to synthesize cyclotetrapeptides. *Org. Biomol. Chem.* **2015**, *13*, 6906–6921.

(21) Gentilucci, L.; Cardillo, G.; Tolomelli, A.; De Marco, R.; Garelli, A.; Spampinato, S.; Spartà, A.; Juaristi, E. Synthesis and conformational analysis of cyclotetrapeptide mimetic  $\beta$ -turn templates and validation as 3D scaffolds. *ChemMedChem* **2009**, *4*, 517–523.

(22) Gentilucci, L.; Cardillo, G.; Spampinato, S.; Tolomelli, A.; Squassabia, F.; De Marco, R.; Bedini, A.; Baiula, M.; Belvisi, L.; Civera, M. Antiangiogenic effect of dual/selective  $\alpha 5 \beta 1 / \alpha v \beta 3$  integrin antagonists designed on partially modified retro-inverso cyclo-tetrapeptide mimetics. *J. Med. Chem.* **2010**, *53*, 106–118.

(23) Clark, J. A.; Pasternak, G. W. US0,488: a kappa-selective agent with poor affinity for  $\mu 1$  opiate binding sites. *Neuropharmacology* **1988**, *27*, 331–332.

(24) Gentilucci, L.; Squassabia, F.; De Marco, R.; Artali, R.; Cardillo, G.; Tolomelli, A.; Spampinato, S.; Bedini, A. Investigation of the interaction between the atypical agonist c[YpwFG] and MOR. *FEBS J.* **2008**, *275*, 2315–2337.

(25) Temussi, P. A.; Picone, D.; Saviano, G.; Amodeo, P.; Motta, A.; Tancredi, T.; Salvadori, S.; Tomatis, R. Conformational analysis of an opioid peptide in solvent media that mimic cytoplasm viscosity. *Biopolymers* **1992**, *32*, 367–372.

(26) Borics, A.; Tóth, G. Structural comparison of  $\mu$ -opioid receptor selective peptides confirmed four parameters of bioactivity. *J. Mol. Graphics Modell.* **2010**, *28*, 495–505.

(27) HyperChem, release 8.0.3; Hypercube Inc. (1115 NW 4th St., Gainesville, FL 32608, U.S.), 2007.

(28) Cornell, W. D.; Cieplak, P.; Bayly, C. I.; Gould, I. R.; Merz, K. M.; Ferguson, D. M.; Spellmeyer, D. C.; Fox, T.; Caldwell, J. W.; Kollman, P. A. A second generation force field for the simulation of proteins, nucleic acids, and organic molecules. *J. Am. Chem. Soc.* **1995**, *117*, 5179–5197.

(29) Piekielek, J.; De Marco, R.; Gentilucci, L.; Cerlesi, M. C.; Calò, G.; Tömböly, C.; Artali, R.; Janecka, A. Redoubling the ring size of an endomorphin-2 analog transforms a centrally acting mu-opioid receptor agonist into a pure peripheral analgesic. *Biopolymers* **2016**, *106*, 309–317.

(30) Perlikowska, R.; Piekielek, J.; Gentilucci, L.; De Marco, R.; Cerlesi, M. C.; Calò, G.; Artali, R.; Tömböly, C.; Kluczyk, A.; Janecka, A. Synthesis of mixed MOR/KOR efficacy cyclic opioid peptide analogs with antinociceptive activity after systemic administration. *Eur. J. Med. Chem.* **2016**, *109*, 276–286.

(31) Gentilucci, L.; De Marco, R.; Cerisoli, L. Chemical modifications designed to improve peptide stability: incorporation of non-natural amino acids, pseudo-peptide bonds, and cyclization. *Curr. Pharm. Des.* **2010**, *16*, 3185–3203.

(32) Janecka, A.; Gentilucci, L. Cyclic endomorphin analogs in targeting opioid receptors to achieve pain relief. *Future Med. Chem.* **2014**, *6*, 2093–2101.

(33) Reichert, J. A.; Daughters, R. S.; Rivard, R.; Simone, D. A. Peripheral and preemptive opioid antinociception in a mouse visceral pain model. *Pain* **2001**, *89*, 221–227.

(34) Labuz, D.; Mousa, S. A.; Schäfer, M.; Stein, C.; Machelska, H. Relative contribution of peripheral versus central opioid receptors to antinociception. *Brain Res.* **2007**, *1160*, 30–38.

(35) Al-Khrasani, M.; Lackó, E.; Riba, P.; Király, K.; Sobor, M.; Timár, J.; Mousa, S.; Schäfer, M.; Fürst, S. The central versus peripheral antinociceptive effects of  $\mu$ -opioid receptor agonists in the new model of rat visceral pain. *Brain Res. Bull.* **2012**, *87*, 238–243.